Vol. 12, No. 3, 2021
ISSN 2233-4203/ e-ISSN 2093-8950
ARTICLE www.msletters.org | Mass Spectrometry Letters

Facile and Rapid Glycosylation Monitoring of Therapeutic Antibodies Through Intact Protein Analysis

Myung Jin Oh[1,2†], Nari Seo[1,2†], JungA Seo[1,2], Ga Hyeon Kim[1,2], and Hyun Joo An[1,2*]

[1]*Graduate School of Analytical Science and Technology, Chungnam National University, Daejeon, Korea*
[2]*Asia-Pacific Glycomic Reference Site, Daejeon, Korea*

Received August 13, 2021, Revised August 27, 2021, Accepted September 08, 2021
First published on the web September 30, 2021; DOI: 10.5478/MSL.2021.12.3.85

Abstract: The therapeutic antibody drug market has experienced explosive growth as mAbs become the main therapeutic modality for a variety of diseases. Characterization of glycosylation that directly affects the efficacy and safety of therapeutic monoclonal antibodies (mAbs) is critical for therapeutics development, bioprocess system optimization, lot release, and comparability evaluation. The LC/MS approach has been widely used to structurally characterize mAbs, and recently attempts have been made to obtain comprehensive information on the primary structure and post-translational modifications (PTMs) of mAbs through intact protein analysis. In this study, we performed state-of-the-art LC/MS based intact protein analysis to readily identify and characterize glycoforms of various mAbs. Different glycoforms of mAbs produced in different expression cell lines including CHO, SP2/0 and HEK cells were monitored and compared. In addition, the comparability of protein molecular weight, glycoform pattern, and relative abundances of glycoforms between the commercialized trastuzumab biosimilar and the original product was determined in detail using the given platform. Intact mAb analysis allowed us to gain insight into the overall mAb structure, including the complexity and diversity of glycosylation. Furthermore, our analytical platform with high reproducibility is expected to be widely used for biopharmaceutical characterization required at all stages of drug development and manufacturing.

Keywords: intact protein, glycoform monitoring, mass spectrometry, bioterapeutics

Introduction

Monoclonal antibodies (mAbs) are highly effective therapeutics for a variety of indications including cancers, viral infections, and autoimmune diseases.[1] Driven by the patent expiration of blockbuster mAbs, biosimilar are rapidly gaining market share in the pharmaceutical industry.[2] Unlike small molecule drugs, mAbs are large molecules composed of a fragment antigen-binding (Fab) domain and a fragment crystallizable (Fc) region which are inherently heterogeneous in structure due to differences in cell line development and production system.[3,4] Changes in manufacturing process, formulation, and storage can lead to significant micro-heterogeneity of mAbs.[5] Therefore, controlling and characterizing the heterogeneity of primary structure and post-translational modifications (PTMs) in mAbs are essential to understanding their function and ensuring product safety and quality.[6,7]

Glycosylation, which can directly affect the efficacy, immunogenicity, and stability of therapeutic antibodies,[6,8-10] is the most crucial protein PTMs in mAbs. The properties of glycan building blocks on mAb are known to affect Fc-effector function and serum half-life. In particular, high-mannose glycans accelerate blood clearance, resulting in reduced serum half-life.[10-12] Afucosylation of glycan core enhances antibody-dependent cellular cytotoxicity (ADCC), whereas galactosylation of glycan antenna increase complement-dependent cytotoxicity (CDC).[2,14,15] For these reasons, comprehensive characterization of glycosylation is critical for target selection, product design and production, and clinical use of mAbs.

Liquid chromatography/mass spectrometry (LC/MS) with high sensitivity, high selectivity, and high resolution has become an indispensable tool for biopharmaceutical analysis, especially for the characterization of glycosylation.[16-18] MS-based assays for the assessment of glycosylation have advanced tremendously over the past few years. Glycosylation analysis for mAbs can be achieved at different levels such as monosaccharides, released glycan, glycopeptide, and

†These authors contributed equally to this work as co-first authors.
*Reprint requests to Hyun Joo An
https://orcid.org/0000-0001-5847-7483
E-mail: hjan@cnu.ac.kr

intact protein.[19-21] In recent years, intact protein analysis using LC/MS has been widely used for accurate mass measurement and characterization of mAbs due to its superior simplicity and convenience, despite some limitations in obtaining information on glycan structure and site-specific localization.[22-24] In particular, intact mAb analysis allows fast and easy characterization of overall glycosylation with minimal sample preparation without the need for release, enrichment, and purification of glycans or glycopeptides.[19,25,26]

In this study, we monitored and compared various glycoforms of mAbs produced in different expression cell lines including CHO, SP2/0, and HEK cell using intact protein analysis. First, the procedure and conditions of intact protein analysis utilizing UPLC/Q-TOF MS were streamlined and optimized for mAb analysis. Antibody therapeutics were directly analyzed with high sensitivity by MS through on-line desalting by C8 column and separation on a diphenyl column. We qualitatively and quantitatively identified the heterogeneity of glycoforms for each mAb and found that different glycoforms were expressed depending on the expression system even in the case of mAbs with conserved amino acid sequences. We also evaluated the similarity of glycosylation between the originator and the biosimilar of trastuzumab using intact mAb analysis platform. Our highly reproducible and robust platform can be applied to the glycosylation characterization of antibody-based therapeutics such as antibody drug conjugates and bispecific antibodies, as well as other biotherapeutics.

Experimental section

Chemicals and Reagents

Three batches of recombinant trastuzumab originators and biosimilars were obtained from Roche Ins. and Celltrion Inc, respectively. Recombinant infliximab was purchased from Janssen. Monoclonal antibody candidates were obtained from Scripps Korea. Molecular weight cutoff (MWCO) spin concentrator were obtained from Thermo Fisher Scientific (Waltham, MA, USA). Peptide N-glycosidase F (PNGase F) was purchased from New England Biolabs (Massachusetts, USA). All solvents such as water, acetonitrile, and formic acid were LC/MS grade.

Sample Preparation

Using a 10 kDa MWCO spin concentrator, the excipient was removed and the mAb was concentrated. Briefly, the spin column was pre-rinsed with 500 μL of water. Five-hundred micrograms of mAb was dissolved to 500 μL of water, loaded onto a rinsed spin column, and centrifuged at 13,500 g for 4 min. After that, 500 μL of water was added to spin column and centrifuged at 13,500 g for 4 min. This desalting step was repeated 3 times. The final mAb solution was transferred to a tube and dried under vacuum. To obtain N-deglycosylated protein, N-glycans were liberated by PNGase F digestion. Briefly, a glycoprotein was dissolved in a solution of 50 mM ammonium bicarbonate of pH range 7~8 and then treated at 37°C for 20 min in the 400 W microwave after adding 2 μL of PNGase F.

LC/MS Analysis

Dried mAb was reconstituted, diluted 10-fold with water, and analyzed using an Agilent 1290 infinity liquid chromatography (LC) system coupled to an Agilent 6550 iFunnel Q-TOF MS (Santa Clara, CA, USA). An Agilent zorbax 300SB-C8 guard column (5 μm, 2.1 mm i.d., 12.5 mm length) and zorbax RRHD diphenyl column (1.8 μm, 2.1 mm i.d., 100 mm length) was used for LC separation. Upon injection of 2 μL of the sample (corresponding to 100 ng protein), mAb was chromatographically separated using 30 min binary gradient consisting of solvent A of 100% water with 0.1% formic acid (*v/v*); solvent B of 100% acetonitrile with 0.1% formic acid (*v/v*) at a flow rate of 0.4 mL/min. The LC gradient used was as follows: 0–3 min, 3% B; 3–14 min, 3–95% B; 14–17 min, 95% B; 17–18 min, 95–3%, B; 18–20 min, 3–95% B; 20–22 min, 95–3% B; 22–24 min, 3–95 % B; 24–26 min, 95–3 % B; 26–30 min, 3 % B. MS was operated in positive extended mass range (2 GHz) mode with scan rate for 1 spectra/second from 500–5,500 *m/z*. The optimal parameters used were as follows: drying gas (N_2) temperature 290 °C, drying gas flow rate 14 L/min, sheath gas (N_2) temperature 350 °C, sheath gas flow rate 12 L/min, nebulizer pressure 20 psi, capillary voltage 5,000V, and fragmentor voltage 300 V. After data acquisition, raw MS spectra were deconvoluted using data processing application program Agilent MassHunter software equipped with BioConfirm.

Results and Discussion

Workflow for glycoform monitoring of mAbs through intact protein analysis

Intact protein analysis is the most straightforward tool in biopharmaceutical development and production as it can intuitively provide the information needed for in-depth insight into the complexity and diversity of glycosylation in biotherapeutics. Workflow based on LC/MS platform for rapid monitoring of glycosylation of mAbs through intact protein analysis was streamlined and optimized as shown in Figure 1A. First, excipients (or detergents) in mAbs that could cause ion suppression during MS analysis or alteration of stationary phase surface chemistry during LC separation were removed by spin column. The mAbs were then directly analyzed by LC/MS equipped with a diphenyl column after C8 on-line desalting. To monitor glycan heterogeneity more clearly, we first deconvoluted multiple charge spectrum into zero charge spectrum and determined various glycoforms based on the exact mass of the paired glycans with amino acid sequence. In general, mAbs produced in recombinant expression systems have

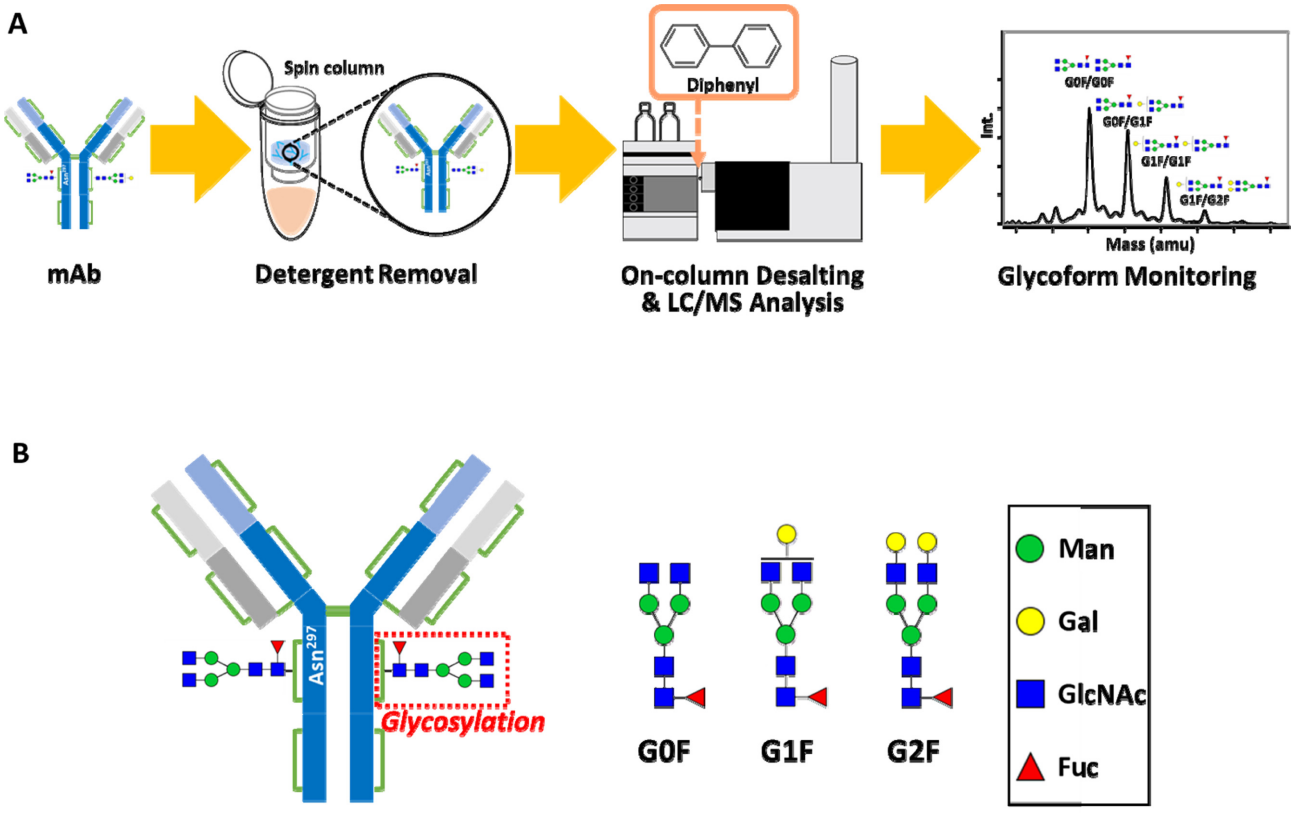

Figure 1. Glycoform monitoring of mAbs through intact protein analysis (A) Schematic illustration of a streamlined workflow (B) Representative glycans found in mAb (G0F, G1F, and G2F).

predominant glycoforms of G0F, G1F, and G2F and a paucity of sialylated glycans, representative glycans are shown in Figure 1B. Note that glycoforms were annotated primarily considering representative glycans of the mAb.

For better understanding of the data processing procedure, a representative multiple charge spectrum and zero charge spectrum generated through the deconvolution process are shown in Figure 2. Raw spectrum of ionized mAb by high-resolution ESI-MS containing multiple charge distributions from 40 to 74 at *m/z* 2000–3600 was converted to zero charge spectrum by deconvolution. Additionally, analysis of N-deglycosylated mAb using PNGaseF allowed us to eliminate glycosylation complexity and determine the molecular weight of non-glycosylated protein corresponding to the mAb backbone. Indeed, the difference between the mass values of the intact protein and N-deglycosylated protein corresponds to the molecular weight of glycoforms of the mAb. For example, the glycan composition of $Hex_7HexNAc_8Fuc_2$ (G0F: 1445.35 Da and G1F: 1607.49 Da) was determined from the difference between the mass values of the intact mAb (148,223 Da) and the N-deglycosylated mAb (145,172 Da). Taken together, multiple peaks in intact protein analysis are due to the diversity and complexity of glycosylation caused by diverse glycans. Glycan configurations such as galactosylation, branching, fucosylation, or sialyation (NeuAc or NeuGc) were identified through sequential correlations mapping linked by the mass of each monosaccharide. As a result, we were able to identify major glycoforms of the mAb, such as G0F/G0F, G0F/G1F, G0F/G2F or G1F/G1F combinations.

Reproducibility and robustness of intact mAb analysis

To ensure the reliability of intact mAb analysis, the reproducibility of intact protein assays was determined using a commercial trastuzumab product as a standard model antibody. Figure 2B presents 20 overlaid deconvolutional mass spectra analyzed by intra and inter days for the trastuzumab intact protein. Interestingly, dozens of mass spectra of trastuzumab were superimposed into one mass spectrum, allowing intuitively high repeatability without statistical processing. Since the ultimate goal of this study is rapid glycosylation monitoring through intact mAb analysis, we calculated pairwise Pearson correlation coefficients (*R*) using the

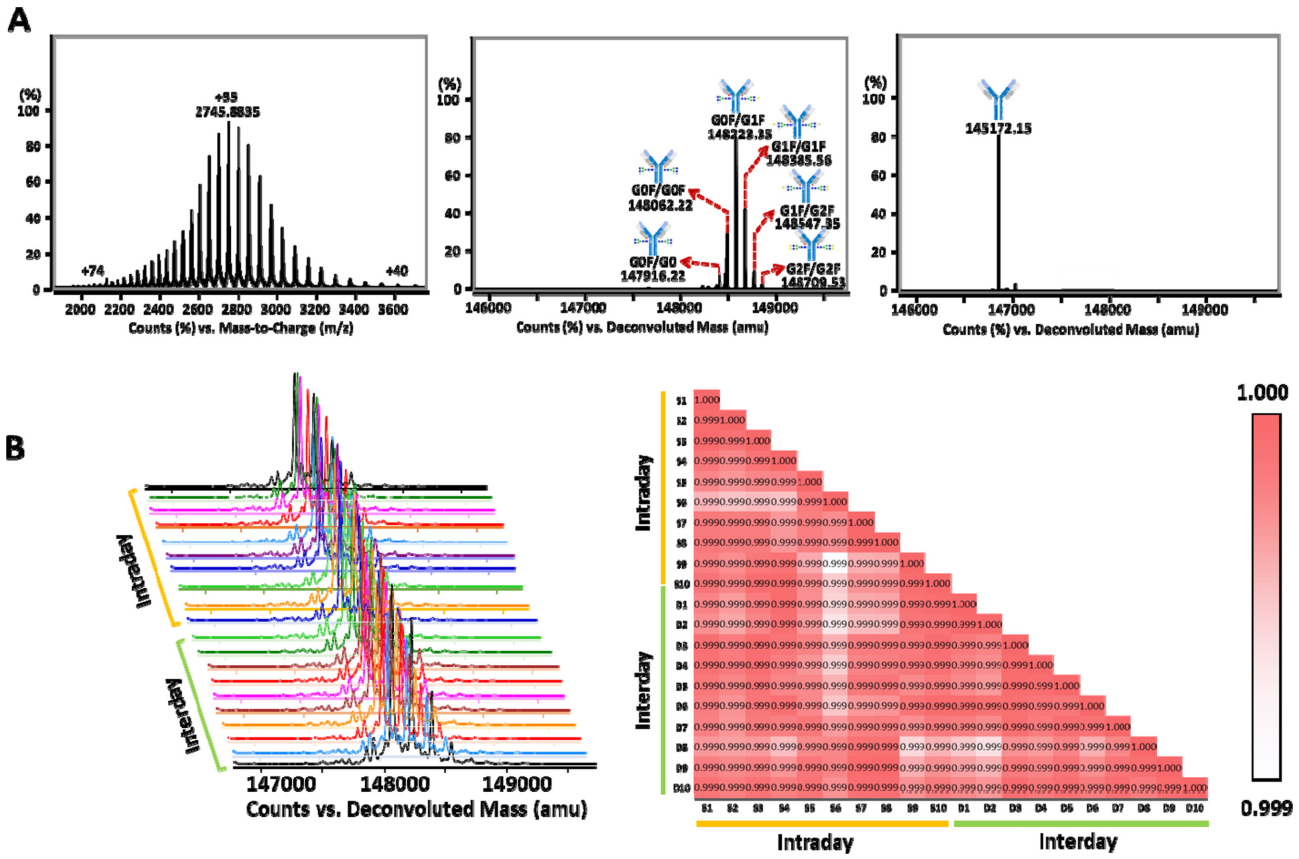

Figure 2. (A) MS Data processing procedure for glycoform identification of mAb. Left: Representative raw mass spectrum with multiple charge state distribution; Middle: Deconvoluted mass spectrum of intact mAb; Right: Deconvoluted mass spectrum of N-deglycosylated mAb (B) Reproducibility of intact mAb assay. Left: 20 overlaid deconvoluted mass spectra obtained from intact analysis of commercial trastuzumab. Right: Correlations between glycoforms of trastuzumab analyzed on different days. An amount of sample corresponding to 100 ng of trastuzumab was injected.

normalized abundances of the four major glycoforms (G0F/G0F, G0F/G1F, G1F/G1F, and G1F/G2F) which account for more than 90% of the total glycoforms abundance in each independent data. All Pearson's *R*s were greater than 0.999 (nearly 1.000), suggesting that high quantitative reproducibility of glycosylation could be achieved in the entire assay. The major glycoform (148,223 Da) with G0F/G1F glycan composition was obtained identically in all 20 deconvolution spectra. Daily variations in MS analyses were within highly acceptable range. In particular, the high reproducibility between 10 MS data obtained on the same day and 10 MS data measured on different days suggests that our platform has high reliability and robustness.

Assessment of glycoform heterogeneity of different mAbs

Host cell lines, growth and expression conditions, and media composition can affect glycosylation of therapeutic antibodies. The mAb has two light and two heavy chains connected by disulfide bonds and consensus N-glycosylation site in the Fc region of heavy chains occupied with complex N-linked glycans with fucose and sialic acid. Various mAbs having the same amino acid sequence but produced in different cell lines were analyzed to confirm glycoform variation according to cell lines (Figure 3). Several glycoforms with different glycan combinations were readily determined from each mAb. After deconvolution, the major peaks were assigned preferentially based on the mass difference of the glycan residues. In Figure 3A, the base peak (148,062 Da), the most abundant glycoform of trastuzumab produced in CHO cells, is theoretically possible only with a glycan composition consisting of $Hex_6HexNAc_8Fuc_2$ (G0F/G0F) within 20 ppm mass error. Consecutive peaks based on the identified major glycoform were specified by examining the mass shift of sugar chains such as galactose (G, 162 Da), GlcNAc (203 Da), and fucose (F, 146 Da). As a result, the remaining peaks were assigned as G0F/G1F, G1F/G1F, G1F/G2F, G2F/G2F, G0F/G0F-GlcNAc, and G0F/G0

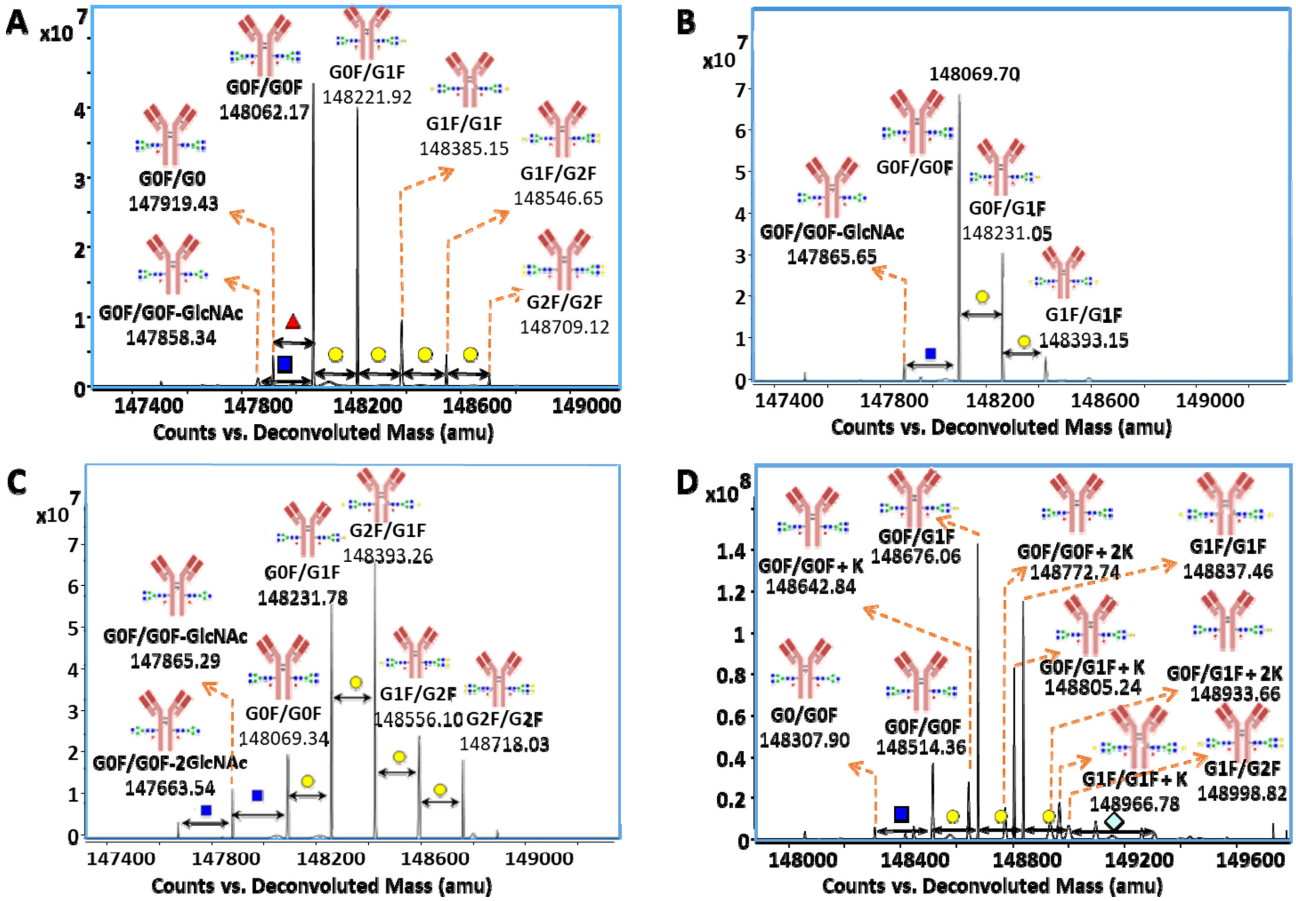

Figure 3. Representative deconvoluted mass spectra of mAbs expressed in different cell lines. Identified glycoforms were annotated. See Figure 1B for information on the glycan structure. (A) Trastuzumab produced in CHO cell; (B) mAb candidate produced in CHO cell; (C) mAb candidate produced in HEK cell; (D) Infliximab produced in SP2/0 cell.

glycoform. The glycoforms of other antibodies were also identified in the same manner (Figure 3B-3D). Interestingly, monoclonal antibody candidates expressed in different cell lines such as CHO cell and HEK cell show different glycoforms (Figure 3 B, C). The major glycoform of mAbs produced in CHO cell was G0F/G0F, whereas the glycoform with the highest intensity of mAbs produced in HEK cell was identified as G1F/G1F. In addition, more galactose capping patterns, such as G1F/G2F and G2F/G2F, were more predominantly observed in mAb expressed in HEK cell. For infliximab produced in SP2/0 cell, the most prominent glycoform was the variant containing G0F/G1F glycoform in both Fc regions as shown in Figure 3D. Unlike other mAbs, specific modifications such as NeuGc sialic acid and C-terminal lysine variants were also detected in infliximab. The glycoforms identified in the commercial products trastuzumab and infliximab and their molecular weights and relative abundances are summarized in Table 1. These results clearly suggest that our platform can be a very informative glyco-characterization tool for cell line selection and monitoring of the production environment.

Comparability assessment of glycosylation between biosimilar and originator

Glycoform diversity, overall architecture, and glycosylation similarity between commercially available originator and biosimilar were examined using intact mAb analysis. Qualitative and quantitative equivalence and heterogeneity between originator (product name Herceptin) and biosimilar (product name Herzuma) produced in CHO cell were assessed based on the MWs and relative intensities of the detected glycoforms. Interestingly, as shown in Figure 4A, the qualitative distribution of the biosimilar is the same as the originator, but the quantitative distribution is somewhat different from the originator, indicating that the glycoform expression level is disparate. The most abundant glycoforms are G0F/G0F from the originator and G0F/G1F from the biosimilar. In order to further identify differences in glycosylation between originator and biosimilar, we evaluated

Table 1. List of glycoform composition identified by intact mAb analysis of trastuzumab and infliximab products.

Glycoform	Trastuzumab			Infliximab		
	Observed MW	Normalized Intensity		Observed MW	Normalized Intensity	
		AVE (%)	CV (%)		AVE (%)	CV (%)
G0/G0F-2GlcNAc	147494.76	0.56	6.79	N.D.	N.D.	N.D.
G0F/G0F-GlcNAc	147858.34	1.49	2.15	148307.90	1.89	3.03
G0/G0F	147913.64	3.38	0.87	N.D.	N.D.	N.D.
G0F/G0F	148062.17	24.08	0.42	148514.36	16.31	1.08
G0F/G1F	148221.92	22.19	0.61	148676.06	21.90	1.50
G1F/G1F	148385.15	9.69	0.39	148837.46	17.46	0.79
G1F/G2F	148546.65	3.98	1.86	148998.82	7.13	5.39
G2F/G2F	148709.12	0.74	6.66	N.D.	N.D.	N.D.
G0F/G0F+K	N.D.	N.D.	N.D.	148644.65	6.13	3.46
G0F/G0F+2K	N.D.	N.D.	N.D.	148772.93	4.58	2.29
G0F/G1F+K	N.D.	N.D.	N.D.	148804.92	11.52	1.52
G1F/G1F+K	N.D.	N.D.	N.D.	148968.17	10.23	2.25
G1F/G2F+NeuGc	N.D.	N.D.	N.D.	149306.70	2.84	2.36

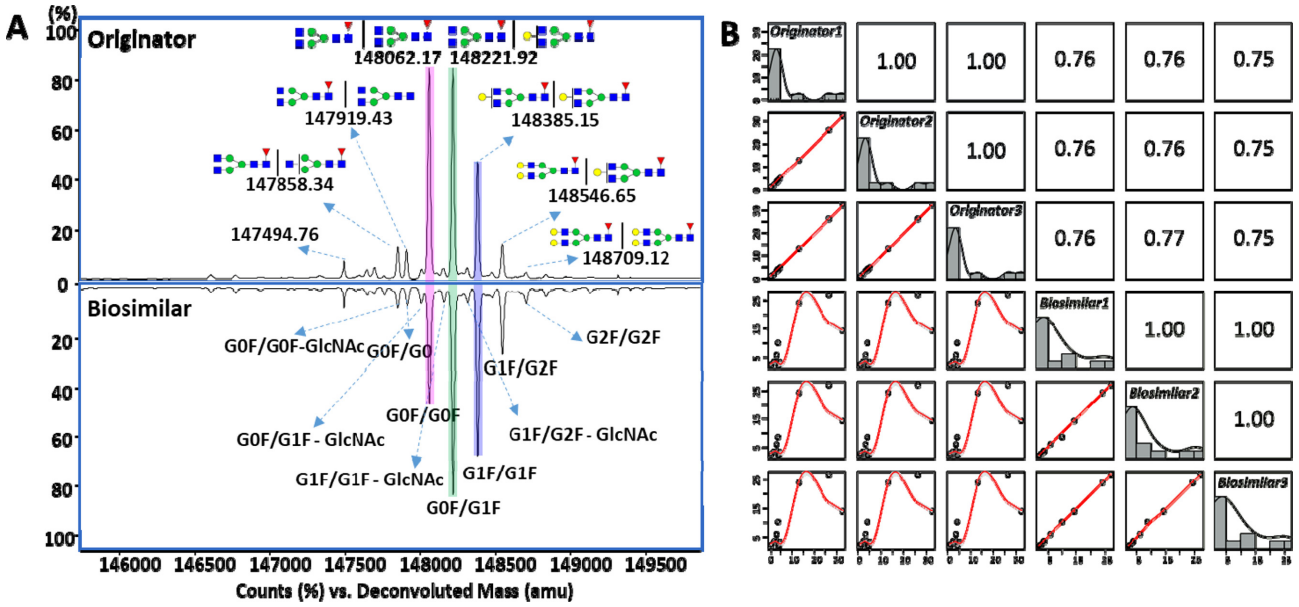

Figure 4. Comparison of glycoproteoform between the originator and biosimilar of trastuzumab. (A) Deconvoluted mass spectra represented as a mirror image. The top panel shows the originator, whereas the bottom panel displays the biosimilar (B) Scatter plot matrix indicates glycoform comparability between original and biosimilar. Diagonal plots are histograms of the relative quantitation of 12 major glycoforms in each mAb with the Pearson correlation coefficients (R) shown above the diagonal.

the relative abundances of three major glycoforms detected in both. The relative ratio of the G0F/ G0F, G0F/G1F, and G1F/ G1F of biosimilar were calculated as 0.5, 1.2, and 2.1 values, respectively, compared to the originator. Each peak was marked with pink, green, and blue, respectively, in the figure for stark comparison. This result means that the galactose capping ratio of trastuzumab, a biosimilar, was significantly higher than that of the originator, suggesting that the biosimilar was decorated with more galactosylation.

Additionally, glycosylation comparability and batch-to-batch variation were simultaneously assessed using intact mAb assays (Figure 4B). Statistical processing was performed using normalized quantitative values for 12 glycoforms commonly detected in all three different batches of originator and biosimilar. Normalized intensity was calculated as the peak intensity of a single glycoform divided

by the sum of peak intensities of all glycoforms detected in the deconvoluted spectrum. The scatterplot matrix shows the glycoform comparability of a total of 6 batches between the originator and the biosimilar. The diagonal plots are histograms of the normalized quantification of 12 glycoforms in each mAb, Pairwise Pearson correlation coefficients (*R*s) were calculated for each pair of batches by plotting the normalized abundance of each glycoform in one batch against the normalized abundance of each glycoform in the other batch in originators and biosimilars (Figure 4B). Batch-to-batch variation in glycosylation is highly positively correlated across all three batches of each product (*R*: 0.99~1), indicating high batch consistency for each product. On the other hand, the *R* value for the glycosylation variation between the original and the biosimilar was estimated to be 0.75 to 0.76, which is thought to be due to the quantitative difference of major glycoforms. These results suggest that product-to-product variation in terms of glycosylation was greater than batch-to-batch variation.

Conclusion

High-throughput analytical tools for biotherapeutic characterization have become essential in the fast-paced biopharmaceutical environment, and fast and robust intact protein analysis is well suited to this need. Here, we demonstrated that consistent information on mAb glycosylation, including glycan composition and glycoform abundance, can be obtained with high reproducibility using intact protein analysis. Furthermore, we have monitored cell line-dependent glycosylation changes, which suggests that our platform will be a very informative glycoform characterization tool for cell line selection, production environment monitoring, and glycosylation comparability assessment within current biopharmaceutical development and manufacturing pipeline. In a situation in which the introduction of artificial intelligence (AI) is being considered for the development and evaluation of biopharmaceuticals, the convergence of AI-technology and MS big data obtained through high-throughput intact protein platform will become a new scientific alternative for complex and intractable glycosylation analysis.

Acknowledgements

This work was supported by the Ministry of Food and Drug Safety(19172MFDS169) and National Research Foundation (2014R1A6A9064166)

References

1. Singh, S.; Kumar, N. K.; Dwiwedi, P.; Charan, J.; Kaur, R.; Sidhu, P.; Chugh, V. K. *Curr. Clin. Pharmacol.* **2018**, 13, 85, DOI: 10.2174/1574884712666170809124728.
2. Grilo, A. L.; Mantalaris, A. *Trends Biotechnol.* **2019**, 37, 9, DOI: 10.1016/j.tibtech.2018.05.014.
3. Beck, A.; Wagner-Rousset, E.; Ayoub, D.; Van Dorsselaer, A.; Sanglier-Cianferani, S. *Anal. Chem.* **2013**, 85, 715, DOI: 10.1021/ac3032355.
4. Jiang, X. R.; Song, A.; Bergelson, S.; Arroll, T.; Parekh, B.; May, K.; Chung, S.; Strouse, R.; Mire-Sluis, A.; Schenerman, M. *Nat. Rev. Drug Discov.* **2011**, 10, 101, DOI: 10.1038/nrd3365.
5. Liu, H.; Gaza-Bulseco, G.; Faldu, D.; Chumsae, C.; Sun, J. *J. Pharm. Sci.* **2008**, 97, 2426, DOI: 10.1002/jps.21180.
6. Zheng, K.; Bantog, C.; Bayer, R. *MAbs* **2011**, 3, 568, DOI: 10.4161/mabs.3.6.17922.
7. Wright, A.; Morrison, S. L. *Trends Biotechnol.* **1997**, 15, 26, DOI: 10.1016/S0167-7799(96)10062-7.
8. Jefferis, R. *Nat. Rev. Drug Discov.* **2009**, 8, 226, DOI: 10.1038/nrd2804.
9. Chung, A. W.; Crispin, M.; Pritchard, L.; Robinson, H.; Gorny, M. K.; Yu, X. J.; Bailey-Kellogg, C.; Ackerman, M. E.; Scanlan, C.; Zolla-Pazner, S.; Alter, G. *AIDS* **2014**, 28, 2523, DOI: 10.1097/QAD.0000000000000444.
10. Beck, A.; Wagner-Rousset, E.; Bussat, M. C.; Lokteff, M.; Klinguer-Hamour, C.; Haeuw, J. F.; Goetsch, L.; Wurch, T.; Van Dorsselaer, A.; Corvaia, N. *Curr. Pharm. Biotechnol.* **2008**, 9, 482, DOI: 10.2174/138920108786786411.
11. Vidarsson, G.; Dekkers, G.; Rispens, T. *Front. Immunol.* **2014**, 5, 520, DOI: 10.3389/fimmu.2014.00520.
12. Tsuda, E.; Kawanishi, G.; Ueda, M.; Masuda, S.; Sasaki, R. *Eur. J. Biochem.* **1990**, 188, 405, DOI: 10.1111/j.1432-1033.1990.tb15417.x.
13. Lawson, E. Q.; Hedlund, B. E.; Ericson, M. E.; Mood, D. A.; Litman, G. W.; Middaugh, R. *Arch. Biochem. Biophys.* **1983**, 220, 572, DOI: 10.1016/0003-9861(83)90449-6.
14. Duivelshof, B. L.; Jiskoot, W.; Beck, A.; Veuthey, J. L.; Guillarme, D.; D'Atri, V. *Anal. Chim. Acta* **2019**, 1089, 1, DOI: 10.1016/j.aca.2019.08.044.
15. Ferrara, C.; Grau, S.; Jager, C.; Sondermann, P.; Brunker, P.; Waldhauer, I.; Hennig, M.; Ruf, A.; Rufer, A.C.; Stihle, M.; Umana, P.; Benz, J. *Proc. Natl. Acad. Sci. U. S. A.* **2011**, 108, 12669, DOI: 10.1073/pnas.1108455108.
16. Zhang, Z.; Pan, H.; Chen, X. *Mass Spectrom Rev* **2009**, 28, 147.
17. Oh, M. J.; Hua, S.; Kim, U.; Kim, H.J.; Lee, J.; Kim, J. H.; An, H. J. *Bioanalysis* **2016**, 8, 711, DOI: 10.4155/bio.16.20.
18. Hua, S.; Oh, M. J.; Ozcan, S.; Seo, Y. S.; Grimm, R.; An, H. J. *Trends Anal. Chem.* **2015**, 68, 18, DOI: 10.1016/j.trac.2015.02.004.
19. Oh, M. J.; Lee, S. H.; Kim, U.; An, H. J. *Mass Spectrom Rev* **2021**, *in press*, DOI: 10.1002/mas.21707.
20. Zhang, P. Q.; Woen, S.; Wang, T. H.; Liau, B.; Zhao, S.; Chen, C.; Yang, Y. S.; Song, Z. W.; Wormald, M. R.; Yu, C. F.; Rudd, P. M. *Drug Discov. Today* **2016**, 21, 740, DOI: 10.1016/j.drudis.2016.01.006.
21. Dotz, V.; Haselberg, R.; Shubhakar, A.; Kozak, R. P.; Falck, D.; Rombouts, Y.; Reusch, D.; Somsen, G. W.;

Fernandes, D. L.; Wuhrer, M. *Trends Anal. Chem.* **2015**, 73, 1, DOI: 10.1016/j.trac.2015.04.024.
22. Zhu, W.; Li, M.; Zhang, J. *J. Proteome Res.* **2021**, 20, 270, DOI: 10.1021/acs.jproteome.0c00373.
23. Fussl, F.; Trappe, A.; Carillo, S.; Jakes, C.; Bones, J. *Anal. Chem.* **2020**, 92, 5431, DOI: 10.1021/acs.analchem.0c00185.
24. Wang, G. B.; de Jong, R. N.; van den Bremer, E. T. J.; Parren, P. W. H. I.; Heck, A. J. R. *Anal. Chem.* **2017**, 89, 4793, DOI: 10.1021/acs.analchem.6b05129.
25. Rosati, S.; Yang, Y.; Barendregt, A.; Heck, A.J.R. *Nat. Protoc.* **2014**, 9, 967, DOI: 10.1038/nprot.2014.057.
26. Kellie, J. F.; Tran, J. C.; Jian, W.; Jones, B.; Mehl, J. T.; Ge, Y.; Henion, J.; Bateman, K. P. *J. Am. Soc. Mass Spectrom.* **2021**, 32, 1886, DOI: 10.1021/jasms.0c00270.

